



Photoelectron spectroscopy on the charge reorganization energy and small polaron binding energy of molecular film



Satoshi Kera^{a,b,*}, Nobuo Ueno^b

^a Institute for Molecular Science, Myodaiji, Okazaki 444-8585, Japan

^b Department of Nanomaterial Science, Graduate School of Advanced Integration Science, Chiba University, Inage-ku, Chiba 263-8522, Japan

ARTICLE INFO

Article history:

Received 5 March 2015

Received in revised form 8 July 2015

Accepted 15 July 2015

Available online 13 August 2015

Keywords:

Hopping mobility

Electron-phonon coupling

Hole-vibration coupling

Vibronic satellite

HOMO fine feature

Polaron

Reorganization energy

Relaxation energy

Ultraviolet photoelectron spectroscopy

Organic semiconductor

Pentacene, Perfluoropentacene

ABSTRACT

Understanding of electron-phonon coupling as well as intermolecular interaction is required to discuss the mobility of charge carrier in functional molecular solids. This article summarizes recent progress in direct measurements of valence hole-vibration coupling in ultrathin films of organic semiconductors by using ultraviolet photoelectron spectroscopy (UPS). The experimental study of hole-vibration coupling of the highest occupied molecular orbital (HOMO) state in ordered monolayer film by UPS is essential to comprehend hole-hopping transport and small-polaron related transport in organic semiconductors. Only careful measurements can attain the high-resolution spectra and provide key parameters in hole-transport dynamics, namely the charge reorganization energy and small polaron binding energy. Analyses methods of the UPS HOMO fine feature and resulting charge reorganization energy and small polaron binding energy are described for pentacene and perfluoropentacene films. Difference between thin-film and gas-phase results is discussed by using newly measured high-quality gas-phase spectra of pentacene. Methodology for achieving high-resolution UPS measurements for molecular films is also described.

© 2015 The Authors. Published by Elsevier B.V. This is an open access article under the CC BY-NC-ND license (<http://creativecommons.org/licenses/by-nc-nd/4.0/>).

1. Introduction

Organic semiconductors are molecular solids with specific charge transport properties due to weak intermolecular interaction [1,2]. A key character to find the semiconductive property in a molecular solid is recognized that (i) an electron (hole) is localized at each molecular site as described by a molecular orbital (MO) picture, however (ii) it is in part delocalized in the molecular solid and spills into other materials at the interface even if they contact by weak electronic coupling. The former feature (i) gives some advantages when fabricating molecular devices, because molecular characteristics in gas phase may be conserved in condensed phase by weak intermolecular interaction. As seen in the present progress of organic electronics, one can estimate qualitatively the device performance in accordance to the individual molecular property and can even synthesize a molecular material with a desired function. On the other hand, the latter feature (ii) is indispensable to realize solid-state devices that use charge transport property and

thus very important target to cut deeply into mechanisms of charge transport throughout the device and origins of their elementary steps. Unfortunately, however, origin of the charge transport property is far from being adequately understood [3,4].

To reveal charge transport characteristic of organic materials quantum mechanically/quantum chemically, the precise experiments on the electronic structure not only of gas phase and/or solid phase (single crystal, thin film etc.), but also at various interfaces in devices, including organic-organic and organic-inorganic (metal/semiconductor) contacts are demanded. Requirements of the electronic structure investigation come from at least two motivations. First, the energy-level alignment (ELA) at the interface between different materials plays a key role in charge injection/ejection to another interface material by overcoming the interface barrier height, or by charge (exciton) separation/recombination processes at the interface. The charge injection barrier dominates the transporting charge-carrier concentration (n) in the electrical conductivity. The ELA is described by measuring the binding energy (BE, E_b) from Fermi level (E_F) and/or ionization energy (IE, E_i) by ultraviolet photoelectron spectrum (UPS).

Second, the carrier dynamics related phenomena give also important bases to discuss charge transport property, which is

* Corresponding author.

E-mail address: kera@ims.ac.jp (S. Kera).

related to the charge mobility μ . The hopping mobility is given by the band shape and intensity in the UPS and band mobility is evaluated by the energy-band dispersion in the angle-resolved UPS.

Charge-transfer processes and carrier dynamics in organic solids have been widely studied in various fields. Detailed theoretical descriptions can be found in several reviews [5–9]. According to general microscopic models, total mobility can be expressed as the sum of two contributions, *i.e.*, (i) coherent conduction that dominates band transport at low temperatures and (ii) incoherent conduction that becomes dominant by charge hopping at high temperatures. Important subjects still to be understood are related to molecular and lattice vibrations (phonons) and their coupling to a charge carrier. The electron-phonon interaction depends on the molecular structure and their packing motif and therefore it can impact both molecular site energies and transfer integrals. The overall strength of electron-phonon coupling observed in highly-resolved UPS is given by the relaxation energy between neutral and ionized states, and the reorganization energy associated. In this short review, we describe a recent development in direct measurements of (local) electron-phonon coupling (HOMO hole–molecular vibration coupling) for large functional molecular materials, which will shed light on the incoherent charge hopping property [3,4].

2. How to realize fine feature measurement

As organic molecules consist of light elements, the intramolecular vibration energy is much larger than energies of lattice phonons, and molecular vibrations with larger energies (~ 100 meV) contribute more to reorganization energy (λ). This means that we do not need an ultimate-resolution electron-spectrometer system for measurement in this level of the study. The principal drawback for obtaining high-resolution UPS is that spectral broadening due to film structure is much larger than the vibration energy, *i.e.*, inhomogeneity of molecular film and energy-band dispersion dominates the observed spectral-line width. We thus need to minimize such broadening in UPS. The non-uniform structure of the thin film introduces serious dependence on the position of the ionization energy, which originates from the site dependence of the electronic states and the relaxation energy (polarization energy) between in the final state upon ionization [10,11]. Furthermore, electronic interaction for adsorbed molecule and substrate should be minimized to reduce the appearance of new interface states with different binding energies.

Fig. 1 shows HeI UPS taken for various phases of pentacene (PEN). The spectra for gas-phase (from ref [12]), monolayer (ML) films, amorphous film, and crystal films are compared. The E_b is measured from the Fermi level of the substrate, and the IE is from the vacuum level. In panel (a), the gas-phase spectrum is well reproduced by theoretical calculation instead of vibration satellites. In panel (b), the monolayer (0.3 nm film on HOPG) spectra, where the electron is emitted from flat-lying film, seem to correspond to the gas-phase one at least for top seven orbitals (all are π states), indicating the electronic structure is not largely modified by intermolecular and molecule–substrate interactions. In panel (e), the spectra correspond to those of the amorphous phase, since there is no clear angular distribution of features. Valence bands are broadened comparing with gas-phase spectrum. In panels (c) and (d), the situation is rather complicated. In the spectrum for 10 nm-pentacene prepared on HOPG (panel (c)), forming an oriented polycrystalline film (long molecule axis parallel to the surface) [13], the highest-occupied molecular orbital (HOMO) band peak does not correspond to the gas-phase position if one makes spectrum alignment at other deeper-lying states. In the spectrum for 20 nm-pentacene prepared on SiO₂ (panel (d)), showing ordered polycrystalline film (long molecule axis

perpendicular to the surface) [14–17], additional feature is appeared at the gap between HOMO and HOMO-1(H-1). These large changes in the HOMO band shape are caused by forming energy-band dispersion for well-stacked polycrystalline samples [18,19]. To describe more precisely, the results of angle-resolved UPS (ARUPS) are useful to understand the band shape [13–19]. When we look the spectra in the details very carefully, the figure in a survey view also tells important physics both on the initial state and final state effects in the UPS, which would be (i) the polarization energy depends on the orbital distribution and (ii) the one-electron approximation does not work for energy level calculations of molecular solids [20,21]. The impact of electronic relaxation is also crucial to understand the charge transport in molecular solids. Upon electron(hole) hopping, for example, the remaining electrons response to the hopping electrons (hole). Effects of such a dynamic relaxation should appear in the photoelectron spectrum and can be discussed by a time-dependent many-particle picture, which is beyond the scope of this review.

The origin of the UPS bandwidth for organic solids was discussed extensively until the end of the 70s [22–24]. After the work done by Salaneck *et al.*, [23], the UPS bandwidth of the HOMO state in organic films was considered to have been mainly dominated by the dependence of relaxation (polarization) energy [24] on the site/depth, since it yielded a broadened UPS feature with a full-width-at-half maximum (FWHM) of ~ 0.4 eV. As a result, it was considered that intermolecular energy-band dispersion could not be measured, since the dispersion width may be smaller than the spectral bandwidth due to the dependence of relaxation (polarization) energy [3] on the site/depth. Nowadays, the measurement of band dispersion on an organic material has been successfully achieved in many systems [3], and very recently even for very small band dispersion in a range of a few-tens meV was observed by Yamane *et al.* for phthalocyanine (Pc) films, which thanks to development in the measurement technique and the sample preparation [25,26]. Unfortunately, the measurement of electron(hole)-phonon(vibration) coupling in organic thin films has also been believed to be impossible, although the possibility of molecular vibration contributing to the width of the HOMO band in UPS has been suggested by taking into consideration of the excellent one-to-one correspondence of the valence-band features to those in gas-phase [27], and evidence was found for a tetracene film in an early work on UPS by N. Ueno. [28]. Therefore, gas-phase UPS spectra, where hole-vibration coupling is resolved for HOMO, have been used in theoretical studies of hole-hopping mobility [5,6]. However, there is a serious problem in using the gas-phase spectrum, since the molecules are in more thermally excited states due to the evaporation at higher temperature. We need to measure HOMO hole-vibration coupling at lower temperatures using thin films or adsorbed molecules to discuss hopping mobility.

In **Fig. 2**, the high-resolution HeI UPS of HOMO taken for various phases of PEN are presented. The spectra for gas-phase, monolayer films [29], amorphous film [18,19], and crystal film [18,19] are measured by using the same apparatus (Omicron HIS13 UV lamp with polarizer and VG-CLAM4 analyzer). In the gas spectrum, a very sharp HOMO band is observed and hole-vibration coupling is detected at the high-binding energy side with asymmetric feature. Note that the line shape of gas-phase UPS depends on the instruments as well as the temperature of molecules. Deposition of low-vapor pressure molecules on electrodes of electron analyzer system may cause serious problems on the line shape as seen in **Fig. 2**. Coropceanu *et al.*, reported a spectrum which shows a larger tail shape in the high-kinetic energy side [12], while our newly measured gas-phase UPS is free from it. The high-kinetic-energy tail feature by Coropceanu *et al.* [12] might be produced by an instrumental artifact. The details of a newly constructed gas-UPS apparatus will be described in elsewhere.

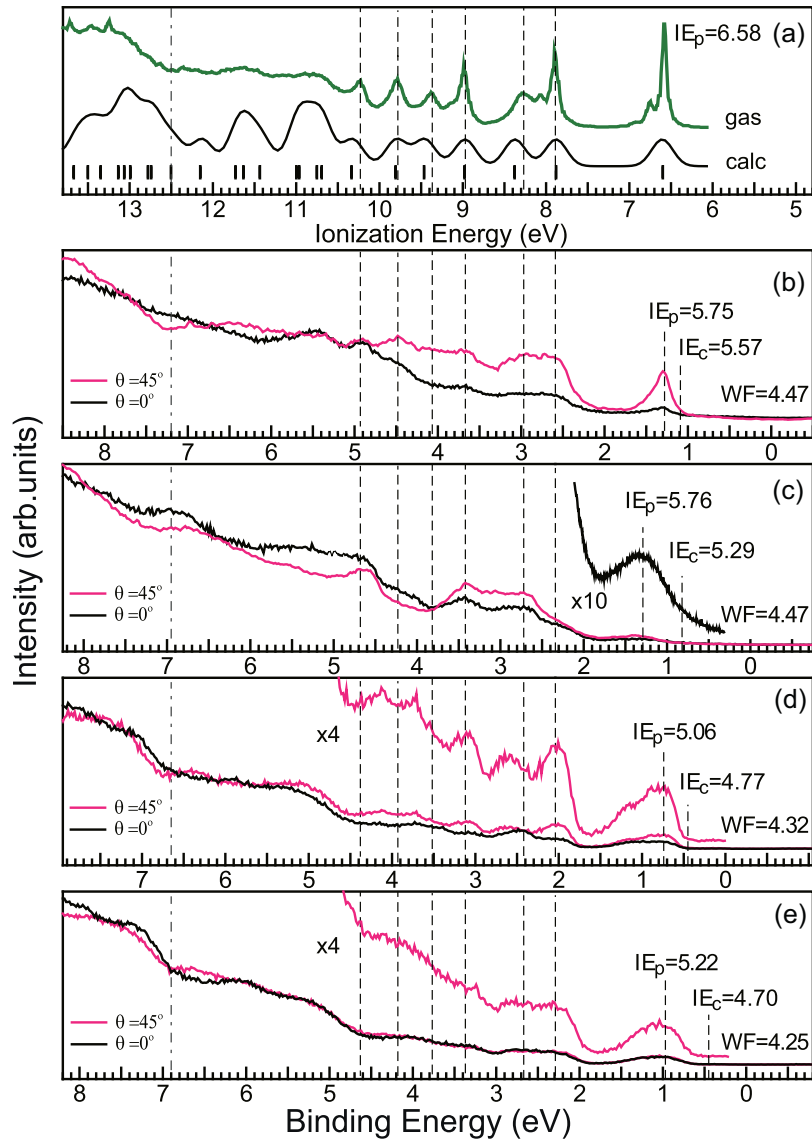


Fig. 1. He I UPS spectra for various phases of pentacene recorded at two different photoemission angles ($\theta = 0^\circ$ (surface normal; black) and 45° (pink/gray)). (a) gas-phase pentacene taken at 508 K reported by Coropceanu et al. [12] and calculated MO energies by a DFT (B3LYP/6-31G**). (b) Flat-lying one-monolayer film (1ML) on HOPG (295 K) [19]. (c) 10-nm pentacene prepared on HOPG (295 K) [19], having an oriented polycrystalline film (long molecule axis parallel to the surface) as described in ref [13]. (d) pentacene(20 nm)/SiO₂/Si(100) [19], showing an oriented polycrystalline film (long molecule axis perpendicular to the surface). (e) pentacene(20 nm)/ITO, giving an amorphous film with molecules of standing tendency. The normal emission spectra are cited from [18,19] and spectra at $\theta = 45^\circ$ obtained for the same sample are newly depicted. The ionization energies of HOMO are measured at the dashed lines; IE_p at the peak and IE_c at the onset energy.

A similar sharp HOMO band is observed for the oriented monolayer film prepared on the HOPG substrate. We will analyze the line shape of this sharp HOMO band and discuss the charge hopping related phenomena. We find important differences in the line shape of the monolayer film depending on the temperature [4,29,30]. On the other hand, a broadened HOMO band with a large tail is observed for the films prepared on the SiO₂ or polycrystalline metal substrates, where the band gives ~ 0.4 eV width and shows no fine features. PEN is known to have polymorphs depending on the condition of film preparation [13], hence two peaks with a sharp onset features [spectrum (e) in Fig. 2] are observed as an evidence of a crystalline sample prepared on CuPc/GeS substrate [19]. These fine features originate from the HOMO band dispersion [14–18].

Organic semiconductor thin films do not grow layer-by-layer to form non-uniform polycrystalline films with a broadened HOMO-band in UPS. Thus, one must prepare a uniform molecular monolayer to attain high-resolution UPS. Although islands of molecules with orientations different to the monolayer region grow

at defects/step bunches of the substrate surface, the islands may be selectively cleaned away by appropriate heat treatment after deposition of a thicker molecular layer, as observed with photoemission electron microscopy (PEEM) [31,32]. From our experience, the detection of vibration satellites with UPS, which appear as skewed asymmetric line shape as seen in Figs. 2 (b) and 2(c), is a good indication of the formation of very large domains of uniform ultrathin organic film. Another important phenomenon during film growth is that molecular thin film changes its packing structure depending on temperature, since intermolecular and molecule-substrate interactions depend on temperature, and this makes it very difficult to prepare a uniform film. Even for ultra-thin films, like a monolayer or bilayer, the packing structure may change depending on the preparation condition that would make a difference in grain size [4,29,33].

When the molecule has a permanent electric dipole, effects of the inhomogeneity in the film appear more clearly in the UPS spectra [34]. We have studied the phenomena for polar-Pc systems

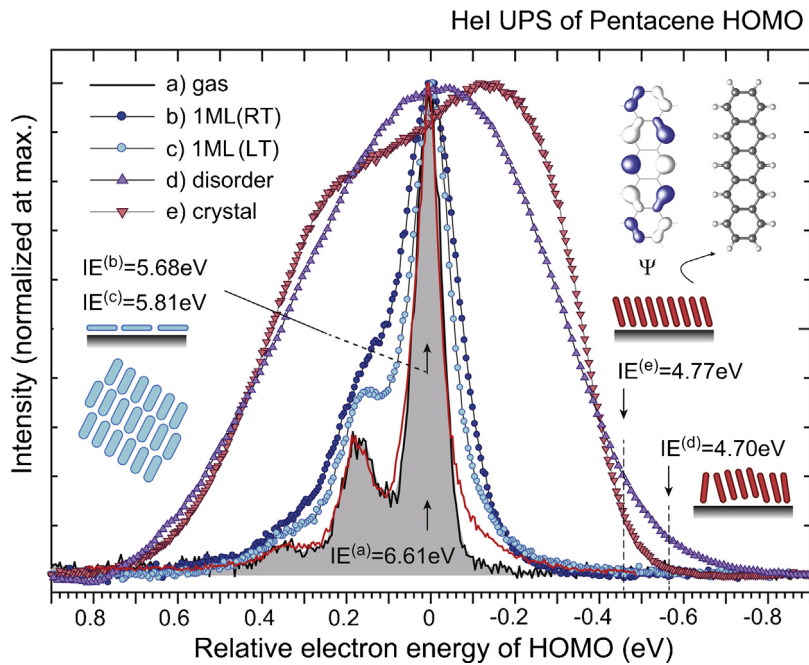


Fig. 2. HeI UPS spectra for various phases of pentacene. (a) gas-phase at 433 K (black curve) by the present measurement and at 508 K (red curve) reported by Coropceanu et al. [12]. (b) lying-monolayer (1ML) on HOPG (295 K, RT) from ref [29], (c) 1ML on HOPG (49 K, LT) from ref [29], (d) standing-disorder ML film (1 nm) on SiO_2 (295 K) from the same sample of ref [19], and (e) standing-crystalline ML film (1.5 nm) on CuPc/GeS (295 K) from the same sample of ref [19]. All spectra are recorded by the same electron energy analyzer and UV lamp. The angle-integrated spectra are shown for the films after subtracting the background signals. The IE of 6.58 eV (gas phase/red curve[12]) is slightly different from the value (IE = 6.61 eV) by our newly measured spectrum (a). The abscissa is aligned to 0–0 transition peak in the gas-phase spectrum. IE for each film ((0–0) peak energy for sharp spectra and onset energy at the dashed line for film spectra) is described in the figure.

(ClAlPc [35], OTiPc [36–39], OVPc [40], and PbPc [36,41]). As an example, HeI UPS of the 0.2-nm-OTiPc/HOPG, the results of the as-grown film on the HOPG kept at room temperature (RT) and the film annealed at 430 K are compared in Fig. 3(b). OTiPc molecule has a permanent electric dipole perpendicular to the molecular plane ($\text{O}^{\delta-}\text{-Ti}^{\delta+}$ direction, 2.16 Debye [38]) with oxygen atom being negatively charged. For the as-grown film, the HOMO band consists of three features denoted by A, B, and C, while a very sharp HOMO band A' is observed for the annealed film as observed in the CuPc/HOPG system [34,39,42]. Similar annealing effects are observed in other polar-Pc systems (ClAlPc, OVPc, and PbPc), which can be explained by the rearrangement of the molecules due to the

diffusion/migration and reorientation of the molecules. The lateral inhomogeneity of the electronic structure due to position dependence of the molecule-substrate interaction is clearly observed with the microspot UPS [10]. The large difference in the UPS features depending on the ensembles would be a general phenomenon for other organic compounds which has a permanent dipole. For some dipole phthalocyanine molecules, monolayers formation on graphite and their dielectric properties are summarized in ref. 39.

On the other hand, a flexibility of the molecular structure at RT is also a key nature of functional molecules. Fig. 4 shows the UPS results for 5,6,11,12-tetraphenyltetracene (rubrene) molecule [43], which attracts high interest, since its single crystals exhibit

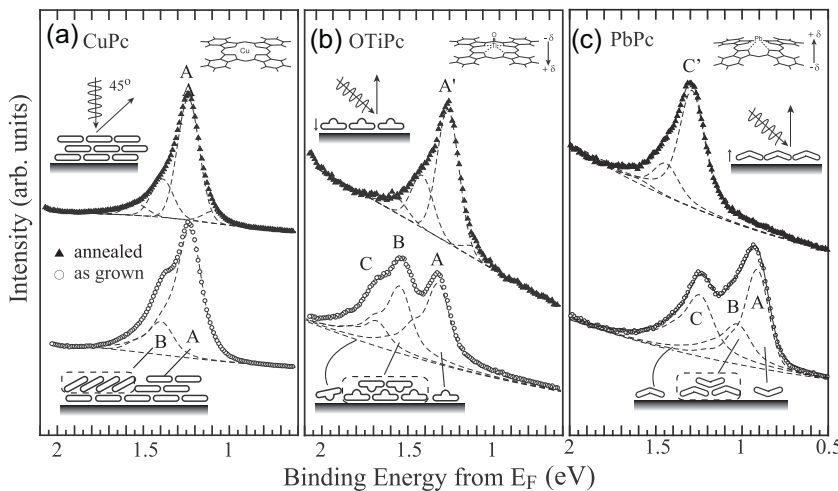


Fig. 3. Effects of annealing on HOMO-band position and width/shape in UPS for (a) CuPc(1 nm)/HOPG, (b) OTiPc(0.2 nm)/HOPG, and (c) PbPc(0.2 nm)/HOPG. Experimental geometry is illustrated in each panel. As-grown film at RT (open circles) and annealed film (filled triangles) are compared. Preparation condition can be found in refs [35–41]. OTiPc and PbPc have an electric dipole as shown in panels (b) and (c), respectively. Corresponding molecular orientations are also shown. The angle between the incidence photon and photoelectron is fixed at 45°. The figure is redrawn from ref [34] with permission.

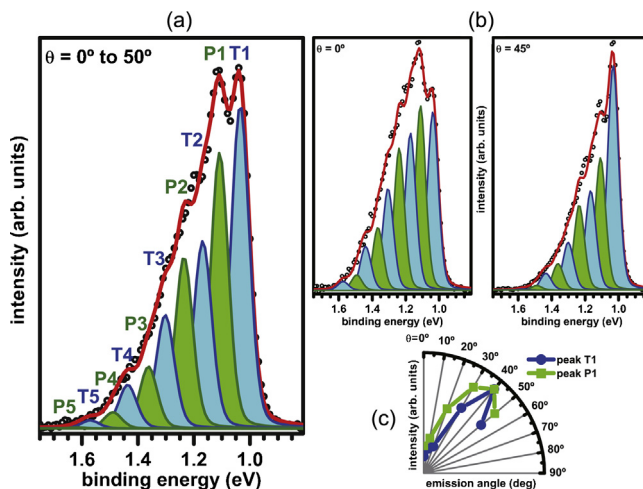


Fig. 4. a) Fitting result to the angle integrated HOMO peak of a monolayer of rubrene on HOPG. Dots correspond to measured data (sum of the background subtracted spectra), cyan/gray peaks to the first ionization peak of the twisted conformation (T) and its vibrational progressions, green/dark gray peaks to the planar conformation (P), and the red line is the sum of the fitted peaks. b) Same for photoemission angles (θ) of 0° and 45° , respectively. c) Photoelectron angular distribution for peak T1 and peak P1 of the rubrene HOMO. The intensities are normalized to the maximum at 40° . The figure is after ref [43] with permission.

very high hole mobility in transistor devices with delocalized band transport [44,45]. Duham *et al* reported that the rubrene monolayer on HOPG consists of two adsorbents of different conformations, so-called twisted and planar structure. Judging from difference of angular distributions of HOMO-band intensity, they successfully deconvoluted the spectral components into two groups from each species. As described later, when we discuss the fine structures or the spectral width/shape of the HOMO band, we should be very careful with the intrinsic/extrinsic inhomogeneity of the prepared film.

As a summary, possible origins of the UPS-band width (shape) due to solid-state effects, which led to the features broadening, can roughly be considered either on (i) a quality of film structure and (ii) intermolecular and/or molecule–substrate interaction. The latter can be classified into four origins: (i) energy–band dispersion, (ii) vibration (phonon) coupling (change in shape), (iii) lifetime broadening (change in shape), and (iv) polarization/relaxation-related phenomena. In principle, the bandwidth of UPS features contains information on electron–phonon coupling, electron (hole) lifetime, and electron–defect scattering. These have been the subjects of an excellent review by Matzdorf [46]. The lifetime broadening in photoemission appears differently from that in an electronic transition to a bound state. The lifetime broadening in photoemission from an ultrathin film of weakly interacting molecules may yield a skewed shape for the line while tailing to a higher kinetic energy, since the photoelectron kinetic energy increases by disappearance of the photo-generated hole potential during existing outside the film [47,48], which is resemble to phenomena due to the post collision interaction (PCI) in gas-phase inner-shell ionization [49,50]. The lifetime of the photogenerated-HOMO hole is dominated by the electronic interaction between ionized molecules and the substrate, also providing information, *e.g.*, on the electron transfer rate from the substrate to the molecule. Note furthermore that the dynamic effects are also related to the time required to polarization/relaxation of ionized molecules and neighboring molecules upon ionization, that is a time series in the various polarons (electronic, very small, small and large polaron) for molecular system [2,51,52]. That is, if the time for polarization/relaxation is in a time scale of a photoelectron to travel to an electron analyzer, the experimental line width (ionization energy) reflects the time

dependence of the polarization/relaxation energy on time. The study on the dynamic polarization, that is polaron phenomena, would open a quantum mechanical view of charge transport in molecular solids [3]. Very recently, we have obtained some evidences on the dynamic effects of charges in the molecular solid by ARUPS measurements (unpublished). The hole-vibration coupling intensity depends on the photoemission angle [4]. It will be an interesting target to study the transport mechanism for organic molecular solids. As a result, the observed UPS spectra show various line shapes.

3. Analysis of electron-phonon coupling

There are two major parameters in hopping transport: (i) the electronic coupling (transfer integral (t)) between adjacent molecules, which needs to be large and (ii) the reorganization energy, λ , which needs to be small to obtain efficient hopping mobility. For hole transport, t can be experimentally obtained from the HOMO-band dispersion of a molecular stacking system [13–17] or by splitting the HOMO level of a dimer molecule [41], though t depends on the overlapping of the necessary wave functions of adjacent molecules [14]. The λ corresponds to the sum of the geometry-relaxation energies (λ_{rel}) when a molecule goes from a neutral to an ionized geometry ($\lambda^{(+)}$) and from an ionized to a neutral geometry ($\lambda^{(0)}$) during hole hopping through molecular aggregates. Since the vibration energies of conjugated C–C stretching modes are 150–200 meV (1200–1600 cm⁻¹), the classical high-temperature approximation is only approximate in hopping transport at room temperature.

If the $\lambda^{(0)}$ does not differ too much from $\lambda^{(+)}$, λ can be written as

$$\lambda = \lambda^{(0)} + \lambda^{(+)} \approx 2\lambda^{(+)} \quad (1)$$

This can be satisfied for a system where the molecular structure is not largely deformed on being ionized. The contribution of each vibration mode to the relaxation energy, $\lambda^{(+)}$, can be determined by the intensities of vibration satellites in high resolution UPS. However the fine features can be accessible only for weakly interacting molecular systems, where $t < \lambda$ is achieved. As demonstrated later, the λ would be a specific parameter of a molecular material, because electron-phonon coupling in large aromatic molecular films is greater for the local molecular vibration than lattice phonons. The relaxation energy of the ionized state, $\lambda^{(+)}$ for hole or $\lambda^{(-)}$ for electron, in the context of small (molecular) polaron theory is also referred to as the polaron binding energy (E_{pol}) here. As E_{pol} is defined as a stabilization energy when the hole is localized on a molecule at a single lattice site, E_{pol} is directly related to $\lambda^{(+)}$. The satellite intensities are described by the values of the Huang-Rhys factors, S , which in harmonic approximation are related to $\lambda^{(+)}$ by

$$E_{\text{pol}} = \lambda^{(+)} = \sum_i S_i h\nu_i \quad (2)$$

where i denotes i -th vibration mode. It is useful to point out that S is directly related to the electron-phonon coupling constant [5,6]. When the neutral state is in the vibrational ground state, the intensities of vibrational progression are given by Poisson distribution

$$I_n = \frac{S^n}{n!} e^{-S} \quad (3)$$

where I_n is the intensity of the n th vibrational satellite. These relationships mean that once the energy of vibration mode i ($h\nu_i$) and corresponding I_n are measured with high resolution UPS of HOMO, S_i , $\lambda^{(+)}$, E_{pol} and λ can be experimentally obtained. The μ can be directly studied by using UPS, since t is also determined

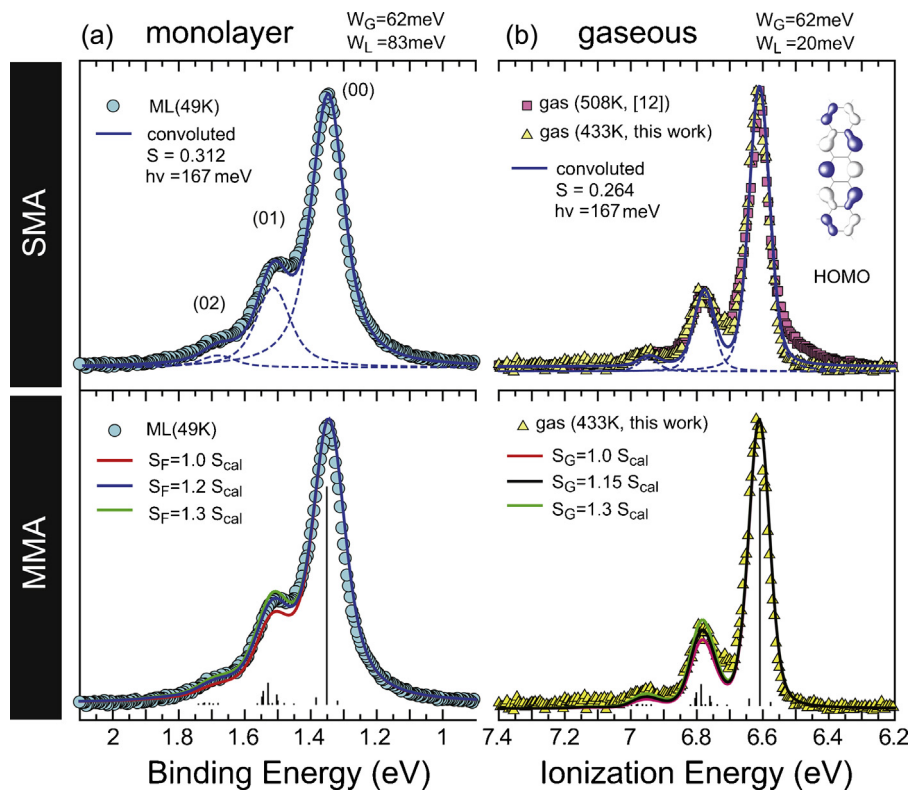


Fig. 5. (a) Angle-integrated-ML UPS spectra (blue circles) for pentacene, compared with convoluted curves by MMA (solid curves) in bottom panel and by SMA (solid curve) in top panel. (b) Newly measured gas-phase UPS spectra (yellow triangles) for pentacene compared with MMA and SMA. Vertical bars in MMA indicate 0-n ($n=0\text{--}4$) transition intensities. Convolution curve in MMA is obtained by Voigt functions ($W_G=62\text{ meV}$ and $W_L=83\text{ meV}$ for ML and $W_G=62\text{ meV}$ and $W_L=20\text{ meV}$ for gas) with S_F (Huang-Rhys factor for film) and S_G (Huang-Rhys factor for gas). The SMA results are shown for convolution with four Voigt functions (the same W_G and W_L to MMAs) with an energy separation ($h\nu$) of 167 meV and $S_F=0.312$ for the ML and $S_G=0.264$ for the gas. HOMO pattern is also shown as inset. The gas UPS spectrum reported by Coropceanu et al is superimposed (pink squares) from ref [12]. Slightly different results of SMA and MMA are reported in ref [30] with different parameter sets that were obtained by comparing gas-phase spectrum of PEN. The ML spectrum is cited from [30] with permission.

by UPS, making the first-principles experimental studies of μ possible [4]. Although these molecular parameters are very helpful in designing organic semiconductor molecules, the high-temperature approximation is too simplistic when we need to calculate μ using experimental λ obtained at low temperatures. Therefore theoretical work is required to realize more effective use of the UPS results in obtaining μ .

Here, we report how to analyze experimental data of the electronic structure and hole-vibration coupling of PEN and perfluoropentacene (PFP) monolayer on graphite [30]. We compare the hole-vibration couplings in PEN and PFP monolayers and in gas phase to study the effect of perfluorination on S_i , $\lambda^{(+)}$, E_{pol} and λ . We observed that the UPS vibrational structure is largely different between PEN and PFP in monolayer phase as well as in gas phase. Furthermore although the vibration energy is decreased by perfluorination as expected from much larger mass of fluorine atom than hydrogen, the vibronic-satellite intensity due to hole-vibration coupling is significantly enhanced in PFP. We found that the latter contribution to λ is much greater than the former one, resulting in serious increase in λ of PFP also for the monolayer.

Hel UPS spectra of the PEN(ML)/HOPG and PFP(ML)/HOPG compared with gas-phase UPS are shown in Figs. 5 and 6, respectively. At first glance one sees that the valence-band features in the monolayer spectra correspond well with those in the gas phase [12,53], indicating the electronic structure is not significantly modified by intermolecular and molecule-substrate interactions. One clearly sees that the HOMO band represents an asymmetric shape caused by a vibrational progression towards the higher E_b side.

3.1. Pentacene (PEN):

We compared UPS spectra, in which the intensity is integrated for photoemission angle $\theta=0\text{--}66^\circ$ after subtracting the background, measured at low temperature of the PEN(ML)/HOPG (at 49 K) and the gas-phase UPS (vaporized at 433 K). The E_b of the gas-phase spectrum is shifted to align the (0-0) peak. The HOMO consists of mainly four fine features, namely a main peak (0-0 vibronic transition) with three satellites (0-1, 0-2, 0-3 vibronic transitions) for the gas-phase and the monolayer spectra. Note that the intensities of the vibration satellites in the 49 K film are more intense than those in the gas phase. We found that such a fine structure shows no coverage dependence during the monolayer formation since the intermolecular interaction along the surface lateral is dominated by the negligibly weak $\sigma-\sigma$ interaction ($\sim 11\text{ meV}$) [54]. These indicate that the hole-vibration coupling in PEN thin films is different from that in free molecules owing to the solid-state effect.

Bredas and co-workers reported that UPS vibrational fine structures of the gas-phase PEN and PFP were well reproduced by using all 18 totally symmetric (A_g) vibrational modes whose intensities satisfy the Franck-Condon principle (linear coupling model) [5,12,53]. Hereafter, we call it multimode analysis (MMA). As described before, there is uncertainty problem in measuring gas-phase UPS for large molecules, hence we demonstrate that the convolution of gas spectrum, which is newly measured by us recently, by MMA using Voigt functions (the FWHM of Gaussian function (W_G) and Lorentzian function (W_L) are fixed to 62 meV and 20 meV respectively) with considering the 0-n ($n=0\text{--}4$) transitions. The width of Voigt function (W_G and W_L) is specified by fitting spectral shape with the low-energy tail of (0-0) peak. Briefly

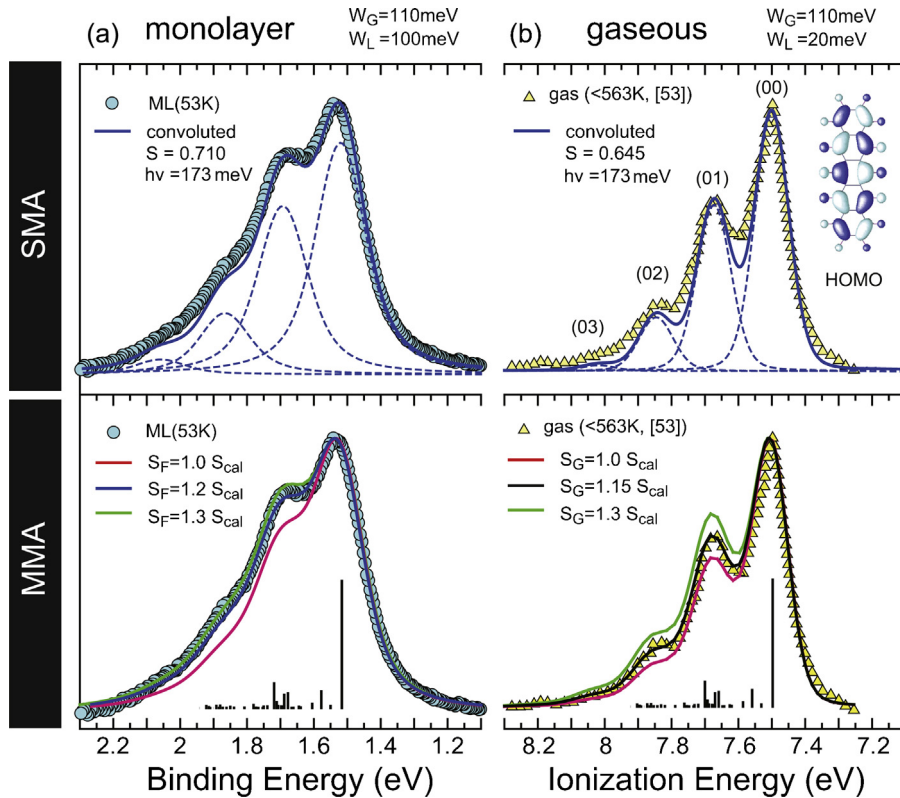


Fig. 6. (a) Angle-integrated-ML UPS spectra (blue circles) for perfluoropentacene (PFP), compared with convoluted curves by MMA (solid curves) in bottom panel and by SMA (solid curve) in top panel. (b) Gas-phase UPS spectra (yellow triangles) for pentacene compared with MMA and SMA. Vertical bars in MMA indicate 0-n ($n=0-4$) transition intensities. Convolution curve in MMA is obtained by Voigt functions ($W_G = 110\text{ meV}$ and $W_L = 100\text{ meV}$ for ML and $W_G = 110\text{ meV}$ and $W_L = 20\text{ meV}$ for gas) with S_F (Huang-Rhys factor for film) and S_G (Huang-Rhys factor for gas). The SMA results are shown for convolution with four Voigt functions (the same W_G and W_L to MMA) with an energy separation ($h\nu$) of 173 meV and $S_F = 0.710$ for the ML and $S_G = 0.645$ for the gas. HOMO pattern is also shown as inset. The gas UPS spectrum by Delgado et al. (green curves) is cited from [53]. The ML spectrum is cited from [30] with permission.

the origin of W_G is from an instrumental resolution and a distribution in the t due to site dependence and/or inhomogeneity of the film, while the origin of W_L , which is necessary to reproduce the tail of the HOMO peak towards the low-energy side, could be described by thermal excitations of vibrations in the initial state of photoionization and/or the finite hole lifetime of the photogenerated hole as described in sec. 2. When one considers the thermal energies of the samples in the measurements, the energy gain is expected to be negligibly small. It is thus considered that the important origin of the large low-energy tail at low temperature is the HOMO-hole lifetime [3,4,47,48].

We used the calculated S factors (S_{cal} : theoretical result for an isolated molecule) and the calculated vibration energies (with a scale factor of 0.9613), for cation state obtained by Brédas et al. to simulate the intensity of vibration satellites. In the present gaseous UPS, which shows much sharper and less tailing feature, we find remarkable disagreement with the simulated curve, even if we assume a Lorentzian contribution to adjust the tail feature. It indicates that the theoretical approximation needs to be further developed even for an isolated molecule. We tried to reproduce the monolayer spectrum by changing the width and S , and found that it shows a better agreement by assuming $S_G = 1.15 S_{\text{cal}}$ (S_G : S for the gas spectrum) than for $S_G = 1.0$ (or 1.3) S_{cal} for each 18-vibrational modes. This analysis yields $\lambda(\text{gas}) = 104\text{ meV}$, $\lambda^{(+)}(\text{gas}) = E_{\text{pol}}(\text{gas}) = 52\text{ meV}$. The pure theoretical values are $\lambda = 92-98\text{ meV}$, $\lambda^{(+)} = E_{\text{pol}} = 46-49\text{ meV}$ [30].

The MMA of monolayer spectrum was performed as the analysis of the gas-phase spectrum by using different Voigt functions ($W_G = 62\text{ meV}$, $W_L = 83\text{ meV}$). The difference in the spectral width and S between gas phase and monolayer phase may be explained by solid

state effects. We found that the convolution using the Voigt functions shows a better agreement by assuming $S_F = 1.2 S_{\text{cal}}$ for each 18-vibrational modes (S_F : S for the film). If we use the instrumental resolution of $W_G = 50\text{ meV}$, the MMA does not agree with the monolayer spectrum (find in [30]). This analysis yields $\lambda(\text{film}) = 108\text{ meV}$, $\lambda^{(+)}(\text{film}) = E_{\text{pol}}(\text{film}) = 54\text{ meV}$ at 49 K as an example. The experimental $\lambda^{(+)}(\text{film})$ is slightly larger than theoretical values of the $\lambda^{(+)}(\text{gas})$. The physical meaning in using a Lorentzian contribution and difference of the Lorentzian contribution between monolayer and gas UPS spectra must be considered in the future.

Instead of the MMA, we describe purely experimental estimation of $\lambda^{(+)} (= E_{\text{pol}})$, where we use only experimental values of the vibration energy and satellite intensity within the available experimental energy resolution, because the present theory cannot explain the gas-phase spectrum perfectly and the MMA is not so easy to handle for a large molecule. Here we call this method as single mode analysis (SMA). Fig. 5 (in the top panels) shows the analysis of angle-integrated UPS spectra of the PEN(ML)/HOPG and the gaseous PEN by the SMA. The spectrum can be reasonably convoluted with the same four Voigt functions as used in the MMA ($W_G = 62\text{ meV}$, $W_L = 83\text{ meV}$ for monolayer and $W_G = 62\text{ meV}$, $W_L = 20\text{ meV}$ for gas) with an energy separation ($h\nu$) of 167 meV assuming a specific vibration mode and $S_F = 0.312$ and $S_G = 0.264$. The SMA results give $\lambda^{(+)} = E_{\text{pol}} = 52\text{ meV}$ for the monolayer at 49 K and $\lambda^{(+)} = E_{\text{pol}} = 44\text{ meV}$ for the gas. The difference to the MMA is larger for gas phase, however the intensities of the vibrational progression follow Poisson distribution in this evaluation, which gives an error less than 10% into $\lambda^{(+)}$ for monolayer film systems. The reorganization energy in the monolayer film is evaluated reasonably.

Table 1

Physical parameters of charge-local phonon coupling obtained for pentacene (PEN) and perfluoropentacene (PFP) for gas-phase and monolayer films.

	MMA				SMA				
	W_G/meV	W_L/meV	S	$\lambda(+)/\text{meV}$	W_G/meV	W_L/meV	$h\nu/\text{meV}$	S	$\lambda(+)/\text{meV}$
PEN ML	62	83	$1.2S_{\text{cal}}$	54	62	83	167	0.312	52
PEN gas	62	20	$1.15S_{\text{cal}}$	52	62	20	167	0.264	44
PFP ML	110	100	$1.2S_{\text{cal}}$	129	110	100	173	0.710	123
PFP gas	110	20	$1.15S_{\text{cal}}$	124	110	20	173	0.645	112

3.2. Perfluoropentacene (PFP):

In Fig. 6 we demonstrate results of the same analyses on PFP(ML)/HOPG (at 53 K) and the gas-phase UPS (vaporized at 503–563 K) obtained by Delgado *et al.* [53]. Similar to the PEN case we found that the gas-phase spectrum cannot be reproduced by the theoretical values and meaningful differences between monolayer and gas-phase UPS. We obtained $\lambda^{(+)}(\text{film}) = E_{\text{pol}}(\text{film}) = 129 \text{ meV}$ for the monolayer at 53 K ($W_G = 110 \text{ meV}$, $W_L = 100 \text{ meV}$, $S_F = 1.2 S_{\text{cal}}$ for 18 modes), while $\lambda^{(+)}(\text{gas}) = E_{\text{pol}}(\text{gas}) = 124 \text{ meV}$ for the gaseous by MMA ($W_G = 110 \text{ meV}$, $W_L = 20 \text{ meV}$, $S_G = 1.15 S_{\text{cal}}$ for 18 modes) (bottom panels). The theoretical values are $\lambda = 181\text{--}232 \text{ meV}$ and $\lambda^{(+)} = E_{\text{pol}} = 91\text{--}117 \text{ meV}$ [30,53]. By SMA, on the other hand, we obtained $\lambda^{(+)}(\text{film}) = E_{\text{pol}}(\text{film}) = 123 \text{ meV}$ for the monolayer ($W_G = 110 \text{ meV}$, $W_L = 100 \text{ meV}$, $S_F = 0.710$, $h\nu = 173 \text{ meV}$), while $\lambda^{(+)}(\text{gas}) = E_{\text{pol}}(\text{gas}) = 112 \text{ meV}$ ($W_G = 110 \text{ meV}$, $W_L = 20 \text{ meV}$, $S_G = 0.645$, $h\nu = 173 \text{ meV}$) for the gaseous, which represent a similar trend as for PEN. We note that the values by the simplest SMA agree fairly well with the complicated MMA. The simplest method of SMA with UPS implies that purely experimental values of $\lambda^{(+)}$, E_{pol} and λ can be used in discussing the hopping charge mobility without using any theoretical computation.

Physical parameters of charge-local phonon coupling obtained by MMA and SMA for PEN and PFP are summarized in Table 1. The λ value of PFP is about two times larger than those of PEN that is in agreement with the results of DFT calculations [30,53], indicating that there is large impact of perfluorination on the HOMO hole-vibration coupling and thus on the transport properties. Furthermore the $\lambda(\text{film})$ values are obviously larger than those estimated from gas-phase UPS and by theoretical calculation for both PFP and PEN probably due to electronic coupling to the substrate and neighbor molecules. This suggests that solid-state effects must be considered for the determination of the electron (hole)-vibration couplings, which is supported by the experimental results that weak intermolecular and molecule-substrate interaction influence the vibrational spectra [55,56]. Note that the large difference between the device mobilities of PFP and PEN involves also contribution of the crystal structure difference of these molecular films [57].

The present results also clearly demonstrate that change in the wave function of HOMO by perfluorination is more critical for hole-vibration couplings and related energy parameters than change in vibration energies, although the substitution of H atoms with heavier F atoms can diminish the vibration energies and thereby contributes to reduce values of these parameters. The difference in the HOMO distributions of PEN and PFP is not very large (see insets in Figs. 5 and 6), but there is contribution of F2p orbital to the PFP HOMO to result in slightly larger HOMO distribution over the molecule. Such a small change in the HOMO yields a significant increase in the HOMO hole-vibration coupling. This again indicates that electron(hole)-phonon(vibration) coupling is more sensitive to the wave function of the responsible electronic state than the phonon energy. The state-of-the-art ARUPS experiments on the orbital tomography can offer an image of the MO distribution [58–62]. Thus it would be very interesting to compare directly, for example, the experimental HOMO distributions of PEN and PFP.

We have observed the UPS-fine features of various organic semiconductor films. A brief summary of the experimental relaxation energies ($= E_{\text{pol}}$) are shown in Fig. 7, where the $\lambda^{(+)}$ estimated by SMA are plotted as a function of the inverse square root of the molecular weight (M). Here, the $\lambda^{(+)}$ for the films were estimated using the spectra recorded at $\theta = 0^\circ$, which may give a larger error for $\lambda^{(+)}$ due to anisotropic angular dependence [4,29]. Nevertheless, we can see clear correlation between the $\lambda^{(+)}$ and the size of the π electron system for oligoacenes (Acs) as has been described in theoretical papers [5,12]. As found in eq. (2), however, the relaxation energy is basically proportional to the coupled molecular vibration energy, indicating the mass of vibrating elements in the HOMO (LUMO) spread may be a reasonable guide parameter to use for decreasing or increasing relaxation energy for positive(negative) molecular charging through electron-phonon coupling.

4. Future aspects

Before closing this short review on UPS fine features to access the charge hopping property, let us compare the results in deeper-lying states, in particular H-1. We investigated the structural and electronic properties of PFP monolayer on Ag(111) substrates using x-ray standing waves (XSW), x-ray diffraction and UPS [63]. XSW results reveal a flat lying geometry of the monolayer PFP/Ag(111) with a relatively large bonding distance of 3.16 \AA for both, the carbon and fluorine atoms, demonstrating weakened π -conjugated plane-Ag(111) interaction. In many cases, π -conjugated molecules

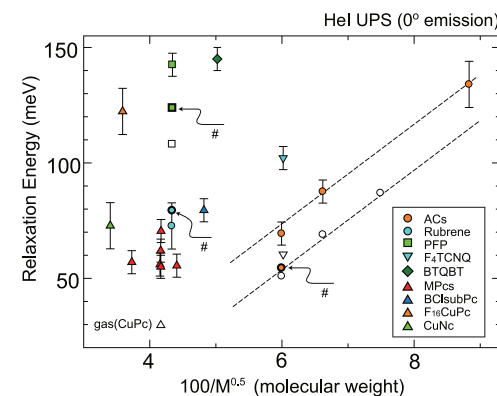


Fig. 7. Updated experimental relaxation energy ($\lambda^{(+)} = E_{\text{pol}}$) vs. $1/M^{0.5}$ (M : molecular weight) for various organic monolayer films. Results are for oligoacene (Ac; pentacene, tetracene, naphthalene), perfluoropentacene (PFP), rubrene, tetrafluoro-tetracyanoquinodimethane ($F_4\text{TCNQ}$), bis(1,2,5-thiadiazolo)-p-quinobis(1,3-dithiole) (BTQBT), metal-phthalocyanine (MPc; $M = H_2, OV, OTi, ClAl, Cu, \text{ and } Pb$), Cu-naphthalocyanine (CuNc), Cu-hexadecafluorophthalocyanine ($F_{16}\text{CuPc}$) and chloro(subphthalocyanato)boron (BCl-subPc). Open symbols are from gaseous-Acs (pentacene, tetracene, and anthracene), PFP, CuPc, and $F_4\text{TCNQ}$. Dashed lines are visual guides. HOMO band measured at normal emission (acceptance angle of 12° deg.) is fitted with Gaussian functions. Single normal mode analysis (typically $150\text{--}170 \text{ meV}$) was considered to determine relaxation energy. Errors are estimated from residual spectra. The SMA results for angle-integrated spectra (PEN, PFP and rubrene) are also plotted by a thick symbol (indicated with #). Some data are obtained from unpublished results.

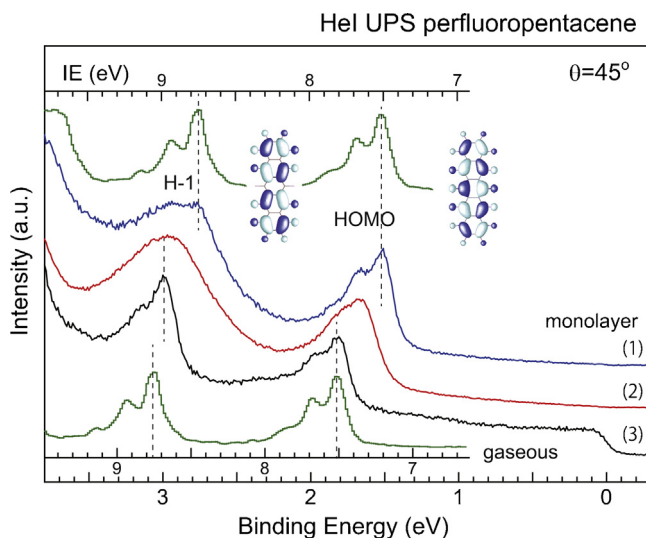


Fig. 8. HeI UPS of perfluoropentacene (PFP) films. (1) monolayer prepared on HOPG and measured at 50 K, (2) at 295 K, and (3) monolayer on Ag(111) at 295 K from ref [63]. All spectra are recorded by VG-SCIENTA analyzer R3000 in angular mode (integrated for 20 deg). The spectrum of PFP on HOPG (1) look slightly different with that in Fig. 6 because the spectra in Fig. 6 was recorded in different analyzer system [30]. The gas UPS spectrum by Delgado et al. (green curves) is cited from [53].

on Ag(111) show a relatively strong interaction and give a charge transfer state [64–66]. The results indicate that fluorination of pentacene significantly reduces the adsorbate-substrate interaction, leading to rather weak interacting (physisorbed) system on other metal surfaces [67,68]. Thus PFP/Ag(111) is a useful prototypical system to investigate the electronic fine structures with less electronic coupling as monolayers-on-graphite systems.

Fig. 8 shows the HeI UPS for PFP monolayer films prepared on the HOPG and Ag(111) substrates to compare the intensity distribution of vibrational fine features as well as the energy gap between the HOMO and H-1. First we compare the vibronic fine features. In the spectrum (3), HOMO and H-1 of PFP/Ag(111) exhibit distinctive vibronic progressions even at RT (295 K). The width of HOMO band profile is rather similar to the gaseous spectrum and very similar to that found for PFP/HOPG at 50 K (spectrum (3)). More interestingly, H-1 of PFP/Ag(111) is sharper than that of the PFP/HOPG at 50 K. We do not have enough data sets necessary for complete analyses of the coupling intensity for this system, namely angle-integrated spectra (by observing many angle-resolved data over a wide angle range), though the difference between the HOMO and H-1 spectra may be related to the solid state effects of orbital distribution on the reorganization energy.

Second we remark the relative energy position of each MO states. As seen in Fig. 8, energy difference between HOMO and H-1, i.e. the energy gap is 1.24 eV for gaseous and monolayer on graphite, but 1.17 eV for monolayer on Ag(111). The reduction of the energy gap at PFP/Ag(111) can be caused by changing the molecule-substrate interaction, hence the study on the following subjects would be interesting; study of (i) changes in the molecular structure upon the adsorption (e.g. deformation of molecular plane), and (ii) dependence of the orbital distribution on the polarization screening. Again the study on the orbital tomography for oriented molecular films using ARUPS [58–62] is very interesting and the study will raise an issue on the limitation of one electron approximation for molecular solids. By adopting comprehensive study on the orbital tomography and vibronic coupling distribution by using state-of-the-art UPS technique, we may push further on the knowledge on an electron in a functional molecular assembly.

5. Summary

Electron(hole)–phonon(vibration) coupling of the HOMO state is studied by using high-resolution UPS for well-ordered ultra-thin films. The reorganization energy and related coupling constants associated with the interaction between holes and molecular vibrations are demonstrated using MMA and SMA of the observed vibronic satellite intensities of the PEN and PFP monolayers. The results indicated that the purely experimental method with SMA is useful for studying the reorganization energy and the charge hopping mobility of organic systems.

Furthermore, we found that the reorganization energy of PFP is significantly greater than that of PEN, which is ascribed to the extended HOMO distribution of PFP by perfluorination of PEN. The comparison with results derived from gas-phase UPS measurements tells importance to realize measurements of gas-phase spectra for large functional molecules by developing an efficient gas-phase UPS apparatus with a high temperature sample cell.

Acknowledgements

The authors are very grateful to Prof. V. Coropceanu, Prof. S. Duhm, Dr. H. Yamane, Dr. H. Fukagawa, and Dr. S. Nagamatsu for stimulating discussions on the computation as well as many students in the Graduate School of Chiba University for doing experiments. The study is partly supported by JSPS KAKENHI (24245034, 20245039, 20685014, 20656002, 17685019), 21st Century COE program (MEXT) and Global COE program (MEXT).

References

- [1] H. Inokuchi, Org. Electronics 7 (2006) 62.
- [2] N. Ueno, Electronic Processes in Organic Electronics: Bridging Nanostructure, Electronic States and Device Properties, in: H. Ishii, K. Kudo, T. Nakayama, N. Ueno (Eds.), Springer Series, Materials Science Vol. 209, Springer, Tokyo, 2015, Chap. 1.
- [3] N. Ueno, S. Kera, Prog. Surf. Sci. 83 (2008) 490.
- [4] S. Kera, H. Yamane, N. Ueno, Prog. Surf. Sci. 84 (2009) 135.
- [5] J.-L. Brédas, D. Beljonne, V. Coropceanu, J. Cornil, Chem. Rev. 104 (2004) 4971.
- [6] V. Coropceanu, J. Cornil, D.A. da Silva Filho, Y. Oliver, R. Silbey, J.-L. Brédas, Chem. Rev. 107 (2007) 926.
- [7] A. Troisi, Chem. Soc. Rev. 40 (2011) 2347.
- [8] F. Ortmann, K.S. Radke, A. Guenther, D. Kasemann, K. Leo, G. Cuniberti, Adv. Funct. Mater. 25 (2015) 1933.
- [9] H. Ishii, Electronic Processes in Organic Electronics: Bridging Nanostructure, Electronic States and Device Properties, in: H. Ishii, K. Kudo, T. Nakayama, N. Ueno (Eds.), Springer Series, Materials Science Vol. 209, Springer, Tokyo, 2015, Chap. 15.
- [10] T. Sugiyama, T. Sasaki, S. Kera, N. Ueno, T. Munakata, Chem. Phys. Lett. 449 (2007) 319.
- [11] T. Sugiyama, T. Sasaki, S. Kera, N. Ueno, T. Munakata, Appl. Phys. Lett. 89 (2006) 202116.
- [12] V. Coropceanu, M. Malagoli, D.A. da Silva Filho, N.E. Gruhn, T.G. Bill, J.-L. Brédas, Phys. Rev. Lett. 89 (2002) 275503.
- [13] N. Koch, A. Vollmer, I. Salzmann, B. Nickel, H. Weiss, J.P. Rabe, Phys. Rev. Lett. 96 (2006) 156803.
- [14] H. Yoshida, N. Sato, Phys. Rev. B 77 (2008) 235205.
- [15] Y. Nakayama, Y. Urugami, M. Yamamoto, S. Machida, H. Kinjo, K. Mase, K.R. Kosswattage, H. Ishii, Jpn. J. Appl. Phys. 53 (2014) 01AD03.
- [16] H. Kakuta, T. Hirahara, I. Matsuda, T. Nagao, S. Hasegawa, N. Ueno, K. Sakamoto, Phys. Rev. Lett. 98 (2007) 247601.
- [17] M. Ohtomo, T. Suzuki, T. Shimada, T. Hasegawa, Appl. Phys. Lett. 95 (2009) 123308.
- [18] H. Fukagawa, S. Kera, T. Kataoka, S. Hosoumi, Y. Watanabe, K. Kudo, N. Ueno, Adv. Mat. 19 (2007) 665.
- [19] H. Fukagawa, H. Yamane, T. Kataoka, S. Kera, M. Nakamura, K. Kudo, N. Ueno, Phys. Rev. B 73 (2006) 245310.
- [20] D.P. Chong, O.V. Gritsenko, E.J. Baerends, J. Chem. Phys. 116 (2002) 1760.
- [21] M. Dauth, M. Wiessner, V. Feyer, A. Schöll, P. Puschning, F. Reinert, S. Kümmel, New J. Phys. 16 (2014) 103005.
- [22] K. Seki, Y. Harada, K. Ohno, H. Inokuchi, Bull. Chem. Soc. Jap. 47 (1974) 1608.
- [23] W.R. Salaneck, Phys. Rev. Lett. 40 (1978) 60.
- [24] W.R. Salaneck, C.B. Duke, W. Eberhardt, E.W. Plummer, H.J. Freund, Phys. Rev. Lett. 45 (1980) 280.
- [25] H. Yamane, N. Kosugi, Phys. Rev. Lett. 111 (2013) 086602.

- [26] H. Yamane and N. Kosugi, J. Electron. Spec. Relat. Phenom. Special Issue: Organic Electronics, in press.
- [27] K. Seki, Y. Harada, K. Ohno, H. Inokuchi, Bull. Chem. Soc. Jap. 47 (1974) 1608.
- [28] N. Ueno, Ph.D. thesis, Tohoku University 1976, in Japanese.
- [29] H. Yamane, S. Nagamatsu, H. Fukagawa, S. Kera, R. Friedlein, K.K. Okudaira, N. Ueno, Phys. Rev. B 72 (2005) 153412.
- [30] S. Kera, S. Hosoumi, K. Sato, H. Fukagawa, S. Nagamatsu, Y. Sakamoto, T. Suzuki, H. Huang, W. Chen, A.T.S. Wee, V. Coropceanu, N. Ueno, J. Phys. Chem. C 117 (2013) 22428.
- [31] M. Shionoiri, M. Kozasa, S. Kera, K.K. Okudaira, N. Ueno, Jpn. J. Appl. Phys. 46 (2007) 1625.
- [32] I. Yamamoto, N. Matsuura, M. Mikamori, R. Yamamoto, T. Yamada, K. Miyakubo, N. Ueno, T. Munakata, Surf. Sci. 602 (2008) 2232.
- [33] T. Kataoka, H. Fukagawa, S. Hosoumi, K. Nebashi, K. Sakamoto, N. Ueno, Chem. Phys. Lett. 451 (2008) 43.
- [34] N. Ueno, S. Kera, K. Sakamoto, K.K. Okudaira, Appl. Phys. A92 (2008) 495.
- [35] S. Kera, H. Yamane, H. Honda, H. Fukagawa, K.K. Okudaira, N. Ueno, Surf. Sci. 566–568 (2004) 571.
- [36] H. Yamane, H. Honda, H. Fukagawa, M. Ohyama, Y. Hinuma, S. Kera, K.K. Okudaira, N. Ueno, J. Electron Spectrosc. Relat. Phenom. 137–140 (2004) 223.
- [37] H. Yamane, H. Fukagawa, H. Honda, S. Kera, K.K. Okudaira, N. Ueno, Synth. Met. 152 (2005) 297.
- [38] H. Fukagawa, H. Yamane, S. Kera, K.K. Okudaira, N. Ueno, Phys. Rev. B 73 (2006), 041302 (R).
- [39] H. Fukagawa, S. Hosoumi, H. Yamane, S. Kera, N. Ueno, Phys. Rev. B 83 (2011) 085304.
- [40] H. Fukagawa, H. Yamane, S. Kera, K.K. Okudaira, N. Ueno, J. Electron Spectrosc. Relat. Phenom. 144–147 (2005) 475.
- [41] S. Kera, H. Fukagawa, T. Kataoka, S. Hosoumi, H. Yamane, N. Ueno, Phys. Rev. B 75 (2007), 121305(R).
- [42] S. Kera, H. Yamane, I. Sakuragi, K.K. Okudaira, N. Ueno, Chem. Phys. Lett. 364 (2002) 93.
- [43] S. Duhm, Q. Xin, S. Hosoumi, H. Fukagawa, K. Ssto, N. Ueno, S. Kera, Adv. Mater. 24 (7) (2012) 901.
- [44] J. Takeya, K. Tsukagoshi, Y. Aoyagi, T. Takenobu, Y. Iwasa, Jpn. J. Appl. Phys. 44 (2005) L1393.
- [45] S. Machida, Y. Nakayama, S. Duhm, Q. Xin, A. Funakoshi, N. Ogawa, S. Kera, N. Ueno, H. Ishii, Phys. Rev. Lett. 104 (2010) 156401.
- [46] R. Matzdorf, Sur. Sci. Rep. 30 (1998) 153.
- [47] H. Hövel, B. Grimm, M. Pollmann, B. Reihl, Phys. Rev. Lett. 81 (1998) 4608.
- [48] A. Tanaka, Y. Takeda, T. Nagasawa, S. Sato, Phys. Rev. B 67 (2003) 033101.
- [49] V. Schmidt, S. Krummacher, F. Wuilleumier, P. Dhez, Phys. Rev. A 24 (1981) 1803.
- [50] T. Miller, T.-C. Chiang, Phys. Rev. B 29 (1984) 1121.
- [51] V. Čápek, E.A. Silinsh, Chem. Phys. 200 (1995) 309.
- [52] E.A. Silinsh, V. Čápek, Organic Molecular Crystals: Interaction, Localization and Transport Phenomena, Springer, Berlin, 1994.
- [53] M.C.R. Delgado, K.R. Pigg, D.A. da Silva Filho, N.E. Gruhn, Y. Sakamoto, T. Suzuki, R.M. Osuna, J. Casado, V. Hernández, J. Teodomiro, L. Navarrete, N.G. Martinelli, J. Cornil, R.S. Sánchez-Carrera, V. Coropceanu, J.-L. Brédas, J. Am. Chem. Soc. 131 (2009) 1502.
- [54] P.B. Paramonov, V. Coropceanu, J.-L. Brédas, Phys. Rev. B 78 (2008), 041403(R).
- [55] K. Fujii, C. Himcinschi, M. Toader, S. Kera, D.R.T. Zahn, N. Ueno, J. Electron. Spectrosc. Relat. Phenom. 174 (2007) 65.
- [56] K. Fujii, S. Kera, M. Oiwa, K.K. Okudaira, K. Sakamoto, N. Ueno, Surf. Sci. 601 (2009) 3765.
- [57] Y. Sakamoto, T. Suzuki, M. Kobayashi, Y. Gao, Y. Funaki, Y. Inoue, F. Sato, S. Tokito, J. Am. Chem. Soc. 126 (2004) 8138.
- [58] P. Puschnig, S. Berkebile, A.J. Fleming, G. Koller, K. Emtsev, T. Seyller, J.D. Riley, C. Ambrosch-Draxl, F.P. Netzer, M.G. Ramsey, Science 326 (2009) 702.
- [59] M. Willenbockel, D. Lüftner, B. Stadtmüller, G. Koller, C. Kumpf, S. Soubatch, P. Puschnig, M.G. Ramsey, F.S. Tautz, Phys. Chem. Chem. Phys. 17 (2015) 1530.
- [60] B. Stadtmüller, S. Schröder, C. Kumpf, J. Electron. Spec. Relat. Phenom. Special Issue: Organic Electronics, in press.
- [61] V. Feyer, M. Graus, P. Nigge, G. Zamborlini, R.G. Acres, A. Schöll, F. Reinert, C.M. Schneider, J. Electron. Spec. Relat. Phenom. Special Issue: Organic Electronics, in press.
- [62] H. Offenbacher, D. Lüftner, T. Ules, E.M. Reinisch, G. Koller, P. Puschnig, M.G. Ramsey, J. Electron. Spec. Relat. Phenom. Special Issue: Organic Electronics, in press.
- [63] S. Duhm, S. Hosoumi, I. Salzmann, A. Gerlach, M. Oehzelt, B. Wedl, T.-L. Lee, F. Schreiber, N. Koch, N. Ueno, S. Kera, Phys. Rev. B 81 (2010) 045418.
- [64] A. Schöll, L. Kilian, Y. Zou, J. Ziroff, S. Hame, F. Reinert, E. Umbach, R.H. Fink, Science 329 (2010) 303.
- [65] B. Stadtmüller, T. Sueyoshi, G. Kichin, I. Kroger, S. Soubatch, R. Temirov, F.S. Tautz, C. Kumpf, Phys. Rev. Lett. 108 (2012) 106103.
- [66] G. Heimel, S. Duhm, I. Salzmann, A. Gerlach, A. Strozecka, J. Niederhausen, C. Bücker, T. Hosokai, I. Fernandez-Torreto, G. Schulze, S. Winkler, A. Wilke, R. Schlesinger, J. Frisch, B. Bröker, A. Vollmer, B. Detlefs, J. Pfau, S. Kera, K.J. Franke, N. Ueno, J.I. Pascual, F. Schreiber, N. Koch, Nature Chemistry 5 (2013) 187.
- [67] N. Koch, A. Vollmer, S. Duhm, Y. Sakamoto, T. Suzuki, Adv. Mater. 19 (2007) 112.
- [68] J.-Z. Wang, J.T. Sadowski, Z.-H. Xiong, Y. Fujikawa, Q.K. Xue, T. Sakurai, Nanotechnology 20 (2009) 095704.